JOURNAL OF MATERIALS SCIENCE 32 (1997) 575–582

Sol–gel synthesis and electrical characterization of (Pb, Ca)TiO_3 thin films

S. CHEWASATN, S. J. MILNE
School of Materials, University of Leeds, Leeds LS2 9JT, UK

Calcium modified lead titanate films have been prepared on Pt/Ti/SiO_2/Si substrates using a sol–gel route. The sols were prepared from propanediol solutions of $Pb(CH_3COO)_2 \cdot xH_2O$, $Ti(OC_3H_7)_2(CH_3COCHCOCH_3)_2$ and $Ca(NO_3)_2 \cdot xH_2O$. Tetragonal phase (Pb, Ca)TiO_3 films could be produced by firing the coatings at 650 °C for 30 min. The limiting thickness of crack-free single layers was ~0.4 μm, but 3 μm thick films could be made by a multiple deposition technique.

Dielectric and ferroelectric parameters were determined for single layer 0.5 μm films for compositions up to 30 mol% Ca. The average values of remanent polarization, P_r and coercive field, E_c decreased with increasing Ca content from ~11 μC cm^{-2} and ~125 kV cm^{-1} for a 10 mol% Ca composition to ~8 μC cm^{-2} and 80 kV cm^{-1} for 30 mol% Ca films. It was noted that the statistical variation in electrical values across each film was greater than in PZT films made by a similar sol–gel route. Reasons for this are discussed in terms of the incidence of physical defects in the films.

1. Introduction

Titanate ferroelectric compositions are under development for device applications such as piezoelectric transducers, memory devices and pyroelectric infra-red sensors. For the latter pyroelectric applications thin films of calcium modified lead titanate, $Pb_{1-x}Ca_xTiO_3$, have attracted some interest [1, 2, 3, 4].

Calcium titanate forms a continuous solid solution series with lead titanate [5, 6, 7]. The present study focuses on compositions containing ≤ 30 mol% Ca. This compositional range exhibits the tetragonal $PbTiO_3$-type structure; substitution of Ca^{2+} for Pb^{2+} reduces the c/a ratio of the parent $PbTiO_3$ unit cell and facilitates ferroelectric switching.

Sol–gel methods for manufacturing thin films of $PbTiO_3$ (PT) and $PbZr_{1-x}Ti_xO_3$ (PZT) are widely reported in the literature, having been originally demonstrated as a convenient fabrication route in the mid 1980s [8, 9]. Mostly, sols are prepared from lead acetate, titanium and zirconium alkoxides and a methoxyethanol solvent. Due to the high reactivity of most of the commonly employed alkoxides, such as $Ti(OC_3H_7)_4$, towards atmospheric moisture [10], the handling procedures and sol reaction sequences are rather complex.

Once formed, by a series of distillation and reflux reactions, the sol is spin-coated onto a substrate and the liquid coating converted to a gel layer by further chemical reaction(s) and solvent evaporation. Finally the sample is thermolysed at up to 600–700 °C in order to eliminate organic components and form a dense crystalline ceramic coating.

With the increasing interest in ferroelectric thin films, alternative sol formulations for $PbTiO_3$ and $PbZr_{1-x}Ti_xO_3$ have been developed [11, 12, 13, 14, 15]. One of these, developed in this laboratory, utilizes a propanediol solution of $Pb(CH_3COO)_2 \cdot xH_2O$, together with titanium and zirconium propoxide reagents which have been chemically modified with acetylacetonate chelating groups.

The handling and processing procedures are more straightforward than for most alkoxide sol–gel systems since the modified alkoxides are more resistant toward atmospheric moisture. In addition the higher viscosity of the coating sols and the assumed greater compliance of the diol gels which make the coatings more resistant to shrinkage stresses enables relatively thick, 1 μm, crack-free layers of PT and PZT to be deposited from a single deposition/firing cycle. The system is thought to form polymeric gels due principally to the bridging of Ti (or Zr) by exchanged propanediol groups, forming linkages of the form $[\text{–Ti–O–}(CH_2)_3\text{–O–Ti–}]_n$ [16]. The route has now been modified to prepare precursor sols for the $Pb_{1-x}Ca_xTiO_3$ system; the structural and electrical properties of calcium modified films made from this propanediol route are reported in this paper.

2. Experimental procedure

The processing scheme for preparing $Pb_{1-x}Ca_xTiO_3$ precursor sols is summarized in Fig. 1. Lead acetate trihydrate, $Pb(CH_3COO)_2 \cdot 3H_2O$, calcium nitrate tetrahydrate, $Ca(NO_3)_2 \cdot 4H_2O$, titanium diisopropoxide bispentanedionate, $Ti(OC_3H_7)_2\,(CH_3COCHCOCH_3)_2$ (TIAA), and propanediol, $HO(CH_2)_3OH$ were used to prepare the precursor solutions. The gravimetrically assayed $Pb(CH_3COO)_2 \cdot 3H_2O$ and $Ca(NO_3)_2 \cdot 4H_2O$

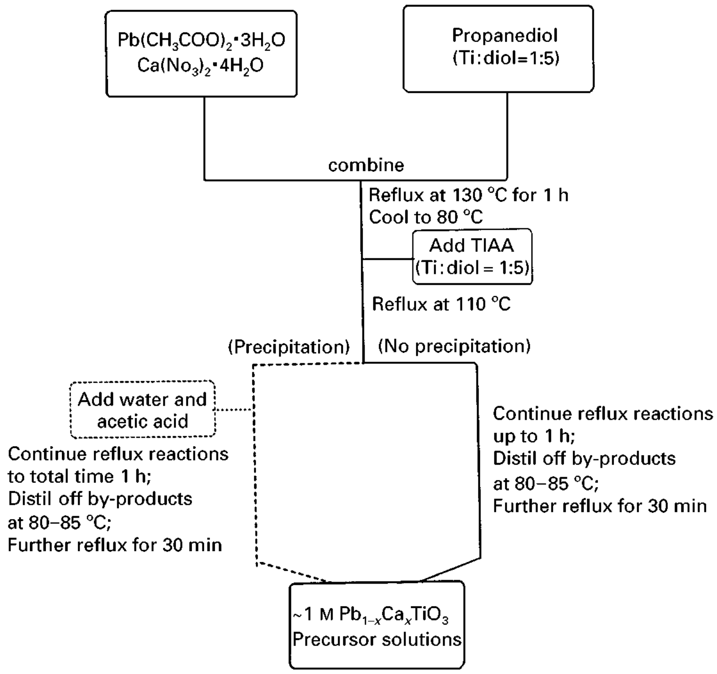

Figure 1 Flow diagram showing principal steps in the synthesis of (Pb, Ca)TiO_3 precursor sols.

reagents were combined in propanediol in a 1:5 molar ratio of (Pb + Ca) to diol, to give various $Pb_{1-x}Ca_xTiO_3$ sol compositions (where $x = 0.05$, 0.10, 0.15, 0.20, 0.25 and 0.30). The solutions were refluxed for 1 h and then cooled to 80 °C prior to adding TIAA. A second reflux was carried out for 1 h with one distillation at ~80–85 °C; approximately 12 vol % of solution was removed at this stage. For sol compositions containing above 20 mol % of calcium, precipitation occurred after the TIAA addition. For the standard quantities of reagents used (TIAA = 14.90 g) it was found that 2.0 ml water and 2.5 ml of acetic acid additions could be used to prevent precipitation. The modified solution was further refluxed for 30 min to promote homogeneity of this solution.

The stock solutions of $x \leqslant 0.15$ compositions had a concentration of ~1.0 M and a density of ~1.3 g cm^{-3}; $0.2 \leqslant x \leqslant 0.3$ stock solutions were prepared to a concentration of ~0.9 M and a density of ~1.1 g cm^{-3}.

The thermal decomposition characteristics of precursor gels were identified using differential thermal analysis (DTA) and thermogravimetric analysis (TGA). Two $Pb_{1-x}Ca_xTiO_3$ samples, $x = 0.10$ and 0.15, were studied. The gels were predried at 150 °C for 3 days and then analysed using a heating rate of 5 °C min^{-1}. To determine crystallization behaviour, the precursor films were prefired on a hot plate at 300 °C for 1 min and then heat treated for 30 min at temperatures from 400 to 700 °C, applying heating and cooling rates of 20 °C min^{-1}. X-ray diffraction (XRD) patterns were recorded using a Phillips APD 1700 diffractometer. The microstructure of as-fired films was studied using scanning electron microscopy (SEM, Hitachi S-700).

For electrical measurements, precursor sols were spin-coated onto cleaned $Si/SiO_2/Ti/Pt_{(111)}$ wafers at 2000 r.p.m. The coated substrates were then pre-fired on a hot plate set at temperatures of 230 or 300 °C for 1 min and fired at 650 °C for 30 min using heating and cooling rates of 20 °C min^{-1}. Top electrodes were prepared by sputtering gold onto the surfaces of the fired films using a metal foil mask to produce an array of 0.7 mm diameter gold dots. Individual dot diameters were measured using an optical microscope fitted with a graticule eyepiece. To make contact with the platinum bottom electrode, a corner of the electroded film was etched away using a 40 vol % solution of fluoroboric acid, HBF_4. Capacitance and dielectric loss measurements were performed at room temperature using an HP 4192A impedance analyser. The measurement was carried out at a frequency of 1 kHz and applied electric field of 2 kV cm^{-1}. The polarization–electric field (P–E) response of the films were examined using a Sawyer–Tower circuit with an applied field of 300 kV cm^{-1} at a frequency of 60 Hz.

3. Results and discussion

The $Pb_{1-x}Ca_xTiO_3$ ($x \leqslant 0.15$) precursor sols were synthesized without any detectable precipitation problems. The sols were stable and remained free of any precipitation over a 6 month period. However, when sols with higher Ca contents $0.20 \leqslant x \leqslant 0.30$ were made using a similar sol preparation procedure to that used for $x \leqslant 0.15$ sols, the sols became cloudy after adding TIAA. The time for precipitation decreased as x increased to 0.3. For example, after adding the TIAA reagent to the $x = 0.20$ solution, evidence of precipitation appeared after refluxing for ~20 min but a precipitate appeared after refluxing $x = 0.30$ sols for only ~5 min. The precipitate was collected and analysed using infrared i.r. spectroscopy; it appeared to be a mixture of calcium acetate and calcium acetylacetonate.

When acetic acid (2.5 ml) and water (2 ml) were added to 30 ml of the cloudy $x = 0.2$ solution, a clear sol was formed once more and the reflux reaction could be continued for a total time of 1 h without any further detectable precipitation. The resulting precursor sol for $x = 0.20$ has remained stable with no detectable precipitation for 6 months, whereas the $x = 0.25$ and 0.30 sols precipitated after standing at room temperature for ~14 days and ~5 days, respectively. Gentle heating caused the latter precipitates to dissolve, but precipitation re-occurred after ~14 days for $x = 0.25$ and ~5 days for $x = 0.30$. Thus fresh precursor sols were generally used to prepare thin films of these high Ca compositions.

The thermolysis behaviour of $x = 0.1$ and 0.15 gels that had been pre-dried at 150 °C is shown in Fig. 2. TGA analysis indicated a major weight loss step ending at ~350 °C and then a smaller weight loss between ~450 °C and ~520 °C, signifying final conversion to a ceramic powder (Fig. 2a).

The DTA data (Fig. 2b), indicated a series of exothermic peaks; those at temperatures between 200 and 350 °C are consistent with the organic pyrolysis steps implied by TGA results. The final DTA peak at ~510 °C is probably due to crystallization of $(Pb, Ca)TiO_3$. The penultimate peaks at ~470 °C may be due to the final pyrolysis of organics and formation of amorphous $PbTiO_3$, and corresponded to the final weight loss in TGA (any intermediate carbonate phase [6] may decompose in this temperature range and so complicate the interpretation of the DTA data).

X-ray diffraction patterns of $x = 0.15$ films deposited from 0.6 M sols on Pt coated silicon substrates that had been heat treated at temperatures from 400–650 °C for 30 min are shown in Fig. 3. Firing at 450 °C resulted in crystallization to a mixture of tetragonal $(Pb, Ca)TiO_3$ and an intermediate pyrochlore phase. The intensity of the pyrochlore peaks decreased as the firing temperature was raised, until at 650 °C no pyrochlore was detected. The phase evolution of other compositions was similar to that of $x = 0.15$.

The variation in lattice parameters as a function of Ca content is shown in Fig. 4. The a-lattice parameter showed only a slight decrease with increasing calcium content whilst the c-lattice parameter noticeably decreased in a non-linear manner by 3.4% over the range $x = 0$–0.3. The relatively high standard deviations may reflect the degree of peak broadening present and of course the low intensity of the peaks in the XRD patterns.

In order to examine the maximum possible thickness of crack-free layers, the effect of sol concentration on film thickness was investigated. Samples were prepared using $x = 0.15$ precursor sols and before determining film thickness all samples were fired at 650 °C for 30 min. A 0.6 M sol produced a crack-free film thickness of ~0.4 μm (Fig. 5a); higher concentrations invariably led to cracking problems. Precursor solutions diluted to 0.4 M were employed for multiple deposition experiments since it was found that higher total thicknesses could be prepared than was the case using 0.6 M sols. The coated substrates were heat-treated on a hot plate at 300 °C for 1 min and then at 650 °C for 1 min prior to repeated depositions. A maximum of ten depositions were possible before cracking occurred. The thickness of these crack-free films made from ten coatings and finally annealed once at 650 °C for 1 h was ⩾ 3 μm, as shown in Fig. 5b. If no 650 °C prefiring treatment was carried out during repeated depositions, it was only possible to deposit a two-layer, 0.8 μm film before cracks appeared. When multiple-layer films were made from 0.6 M sols, again using a two-stage pre-firing sequence, only three layers could be deposited giving a maximum crack-free thickness of ~1.2 μm.

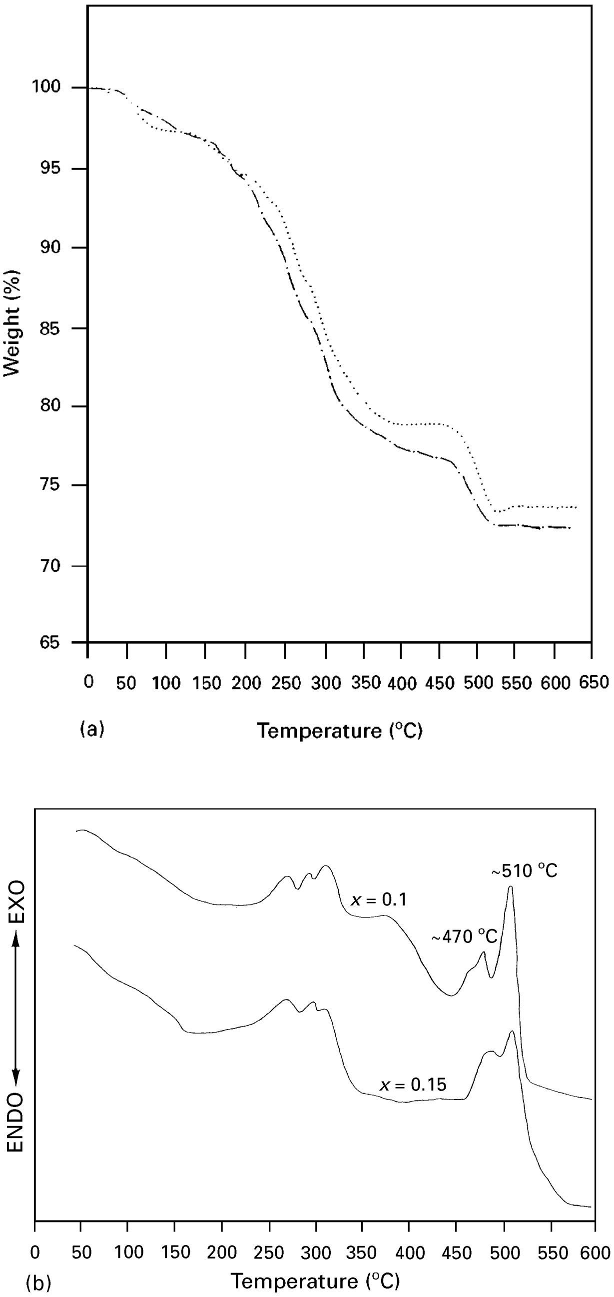

Figure 2 (a) Thermogravimetric analysis data (TGA) for bulk gels of $Pb_{1-x}Ca_xTiO_3$: $x = 0.1$ (····) and 0.15 (–·–). (b) Corresponding DTA data.

The evolution of surface microstructures of ~0.6 μm thick $x = 0.15$ films deposited on Pt coated silicon substrates and heat-treated at temperatures from 500–700 °C is shown in Fig. 6. In films fired at

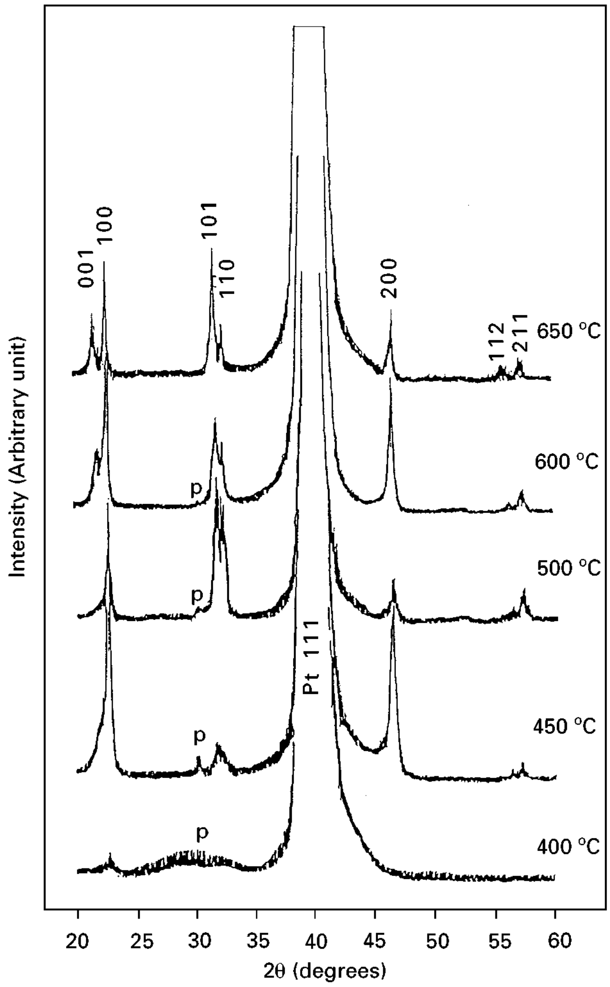

Figure 3 XRD results as a function of firing temperature for $Pb_{1-x}Ca_xTiO_3$: $x = 0.15$ films on platinized silicon substrates (P = pyrochlore).

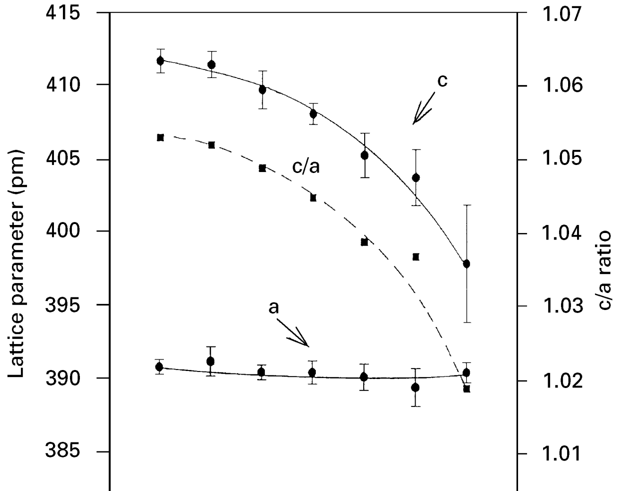

Figure 4 Lattice parameters and c/a ratios for $Pb_{1-x}Ca_xTiO_3$ films.

400 °C for 30 min no resolution of microstructural features was possible; on increasing the firing temperature to 500 °C, grains (or grain clusters) < 0.1 μm in size could be identified (Fig. 6a). At a firing temperature of 600 °C (Fig. 6b), the microstructure of the films clearly displayed the coalescence of small grains, into clusters $\leqslant 0.2$ μm in size with clearly defined pore channels surrounding them. The 500 °C sample may have possessed a similarly clustered grain structure but on too fine a scale to be identified by SEM. When the firing temperature was raised to 700 °C, the grain clusters became larger, $\leqslant 0.5$ μm, and inter-cluster porosity became more apparent (Fig. 6c). However, transmission electron microscopy (TEM) would be required in order to fully characterize the structure of the grain clusters.

The as-fired surfaces of 0.5 μm single-layer films of different $(Pb, Ca)TiO_3$ compositions fired at 650 °C for 30 min, as well as $PbTiO_3$ fired at 700 °C for 30 min were also examined in the SEM (Fig. 7). The as-fired surface of $PbTiO_3$ (i.e. $x = 0$) films exhibited a uniform microstructure of ~0.1 μm grains (Fig. 7a). For $x = 0.10$ films, there was obvious coalescence of $\leqslant 0.1$ μm grains into clusters ranging up to 0.6 μm in size (Fig. 7b). When films were prepared from $x = 0.15$ sols, well-defined clusters were again observed on the film surfaces (Fig. 7c). However, the clusters appeared more dense than those of the same composition fired at a slightly higher temperature (700 °C, Fig. 6c); this may illustrate some of the variations that can arise between different batches. For $x \geqslant 0.20$ fired at 650 °C for 30 min, a further refinement of microstructure was observed with a more dense and fine grained structure than for lower Ca contents (Fig. 7d). The $x = 0.25$ and 0.30 films gave similar microstructures to that shown in Fig. 7d for the $x = 0.2$ sample. These results indicate that increasing levels of substitution of Ca for Pb causes a progressive change in microstructure, with surface microstructure becoming apparently more uniform in density with increasing Ca levels.

Electrical measurements were carried out for ~0.5 μm thick single layer $Pb_{1-x}Ca_xTiO_3$ $(0.10 \leqslant x \leqslant 0.30)$ film specimens after they had been aged for 2 weeks at room temperature. An example of a hysteresis loop for an $x = 0.20$ sample is shown in Fig. 8. Average values of electrical properties were obtained from at least 10 dot electrodes and are plotted as a function of Ca content in Fig. 9. The remanent polarization, P_r (Fig. 9a), generally showed a decreasing trend with increasing calcium concentration. However P_r values ($\sim 10\ \mu C\ cm^{-2}$) for $x = 0.10$ films were slightly lower than those for $x = 0.15$ films ($P_r \sim 14\ \mu C\ cm^{-2}$) but the variability in values within each sample (Table I) creates some doubt as to the significance of this result. No ferroelectric P–E response could be obtained for $PbTiO_3$ and $Pb_{0.95}Ca_{0.05}TiO_3$ films, probably because the switching field lay above the electrical breakdown field. The coercive field, E_c, of all films studied decreased with increasing calcium content from $125\ kV\ cm^{-1}$ for $x = 0.1$ to $\sim 80\ kV\ cm^{-1}$ for $x = 0.25$ and $x = 0.3$. The relative standard deviation in P_r and E_c values and the proportion of electrodes shorting was higher, by a factor of 2–4, than in PZT films made by a diol sol–gel route [14, 18].

The relative permittivity of our Ca–PT films showed no clear trend with changing Ca concentration

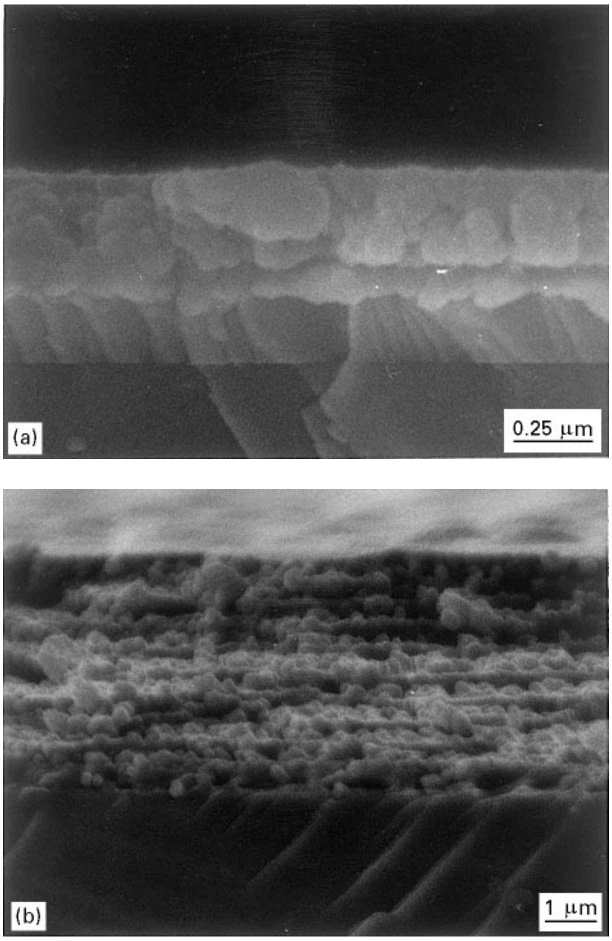

Figure 5 SEM sections showing the thickness of a $Pb_{1-x}Ca_xTiO_3$, $x = 0.15$, film prepared from (a) a single deposition of a 0.6 M sol, and fired at 650 °C for 30 min; (b) ten coating/prefiring steps using a 0.4 M sol fired once at 650 °C for 30 min.

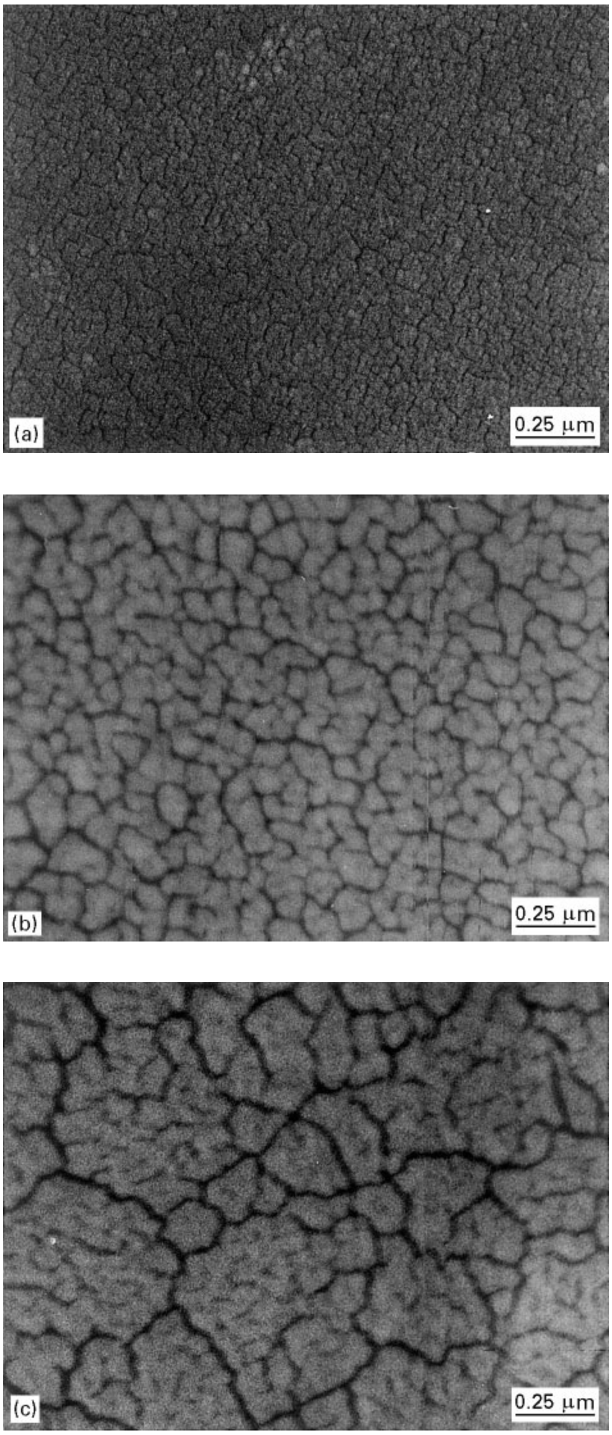

Figure 6 Surface microstructures of a $Pb_{1-x}Ca_xTiO_3$, $x = 0.15$, film fired for 30 min at different temperatures: (a) 500 °C; (b) 600 °C; (c) 700 °C.

(Table I). Around 20% of dots shorted in the various films; of the remainder, there was a relative standard deviation of between approximately 5–10%.

Other workers have reported $Pb_{0.76}Ca_{0.24}TiO_3$ thin films prepared from a sol made from lead acetate, TIAA and propanediol and a solution of calcium acetate in water; the films gave a coercive field E_c of the order of $100\ kV\,cm^{-1}$ and remanent polarization P_r of $\sim 6\ \mu C\,cm^{-2}$ for $\sim 0.7\ \mu m$ thick single layer films [4]. In addition a methoxyethanol sol–gel route has been used to produce 0.1 µm single layers and 1 µm multilayer $Pb_{1-x}Ca_xTiO_3$ films. For 1 µm films, P_r and E_c decreased from $17\ \mu C\,cm^{-1}$ and $230\ kV\,cm^{-1}$ for $x = 0.1$ to $4.6\ \mu C\,cm^{-1}$ and $68\ kV\,cm^{-1}$ for $x = 0.3$ compositions [3].

In later experiments films were pre-fired at 230 °C instead of 300 °C, as in these films, only around 10% of electrode pads measured at high fields resulted in electrical shorting, i.e. a two-fold reduction in failure rate. Structural examination of the films pre-fired at 230 °C indicated a reduced incidence of $\sim < 1\ \mu m$ diameter holes compared to films pre-fired at the higher temperature; examples of these macro-defects are shown in Fig. 10. However even in these improved $(Pb, Ca)TiO_3$ films, macro-defects were a much more serious problem than for $Pb(Zr, Ti)O_3$ films made by a similar route. Sputtering gold top electrodes onto areas of the film containing holes penetrating the depth or most of the depth of the coatings would inevitably cause electrical shorting.

The relatively high variability in measured electrical parameters in electrodes sustaining a sufficient electrical field may arise for similar reasons, i.e. disruption to the surface during decomposition leads to variations in porosity, and hence measured electrical properties, under the dot electrodes.

A hot plate temperature of 300 °C had been initially adopted since it previously had been found to be a suitable temperature for PZT films. Presumably the

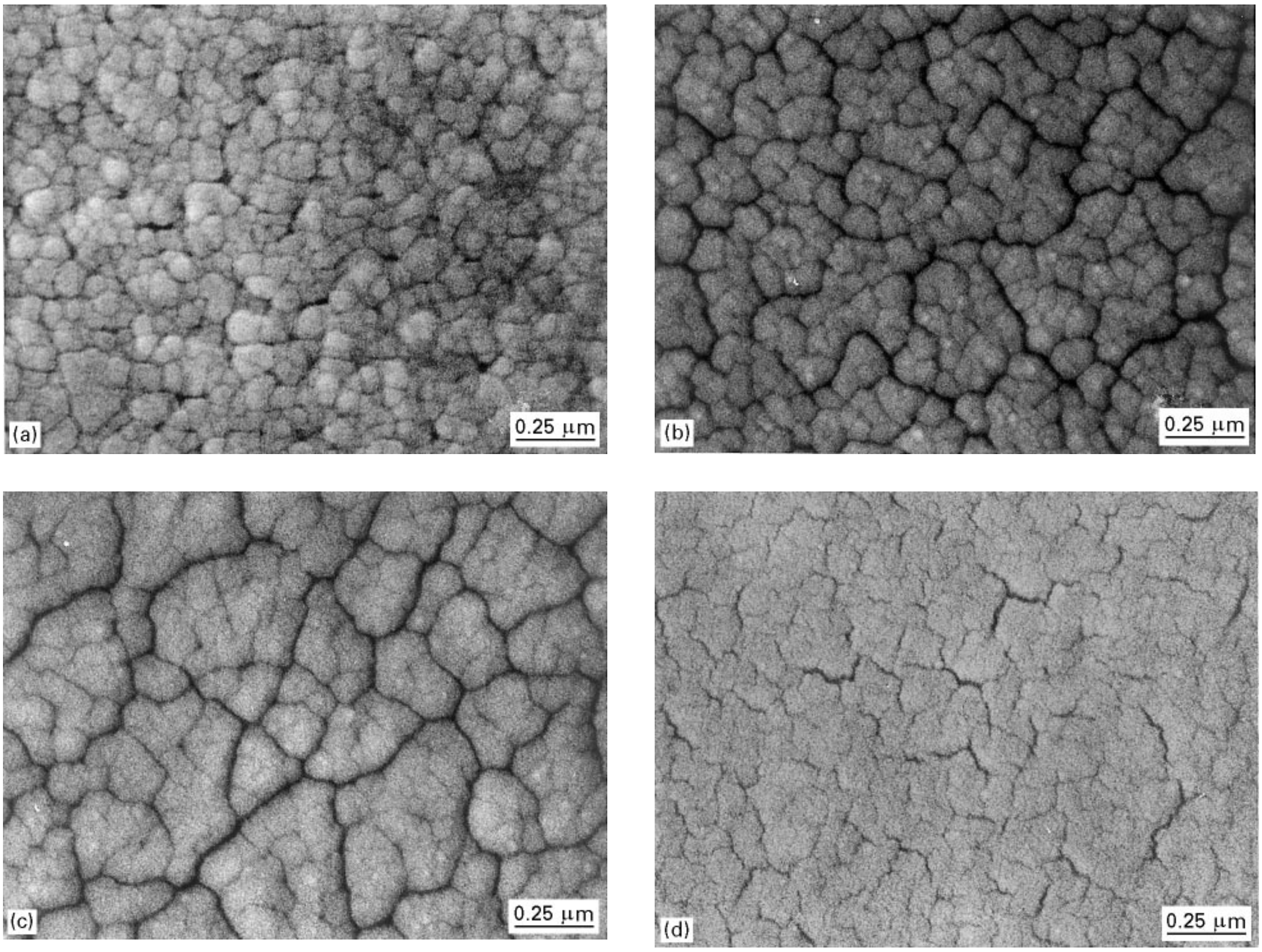

Figure 7 Surface microstructures of $Pb_{1-x}Ca_xTiO_3$ films of different Ca content: (a) $x = 0$ (fired for 30 min at 700 °C); (b) $x = 0.1$; (c) $x = 0.15$; (d) $x = 0.2$ (b–d all fired at 650 °C for 30 min).

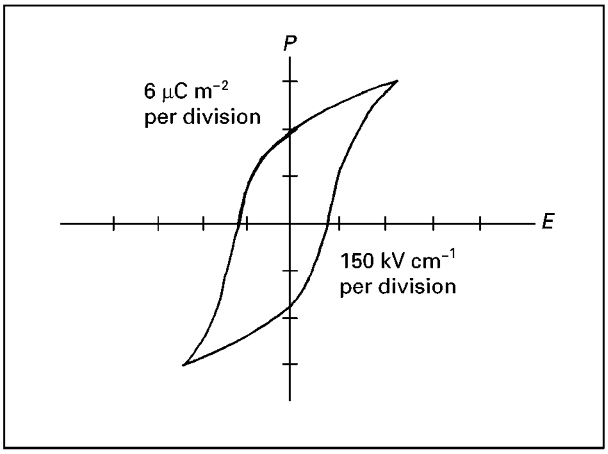

Figure 8 *P–E* hysteresis loop for an $x = 0.2$ film.

$(Pb, Ca)TiO_3$ gels differ in structure and properties to those of $Pb(Zr, Ti)O_3$ and give rise to different optimum hot-plate temperatures.

The incidence of physical defects in the films seemed to increase with increasing levels of Ca. Although the initial problems of precipitation from the stock solutions could be minimized/avoided by water and acetic acid additions, the low solubility of the calcium salt (or its derivative(s)) remained a major concern. The general view held that substitution of calcium acetate for lead acetate led to inferior gel properties. At this stage the origin of the macro-defects is uncertain; phase separation of solvent from the gel and subsequent volatilization from isolated pockets of solvent is one possibility. Alternatively the gel structure may be weaker than for the case of PZT systems, and hence the coatings can be disrupted more easily during the thermal expulsion of organic decomposition products. Given the solubility problems encountered during sol synthesis, precipitation of the calcium species and chemical segregation in the coatings was suspected as another possible cause of the scatter of electrical data, but SEM–energy dispersive analysis of X-rays (EDAX) analysis was inconclusive.

Earlier nuclear magnetic resonance spectroscopy (NMR) investigations on $PbTiO_3$ precursor sols point to the formation of $[Ti–O(CH_2)_3–O–Ti]_n$ polymeric species and it is probable that the lead remains dissolved in solvent trapped within the pores in the gel structure rather than being incorporated directly into the polymer chain. A homogeneous polymeric gel containing both elements in the polymer chain would be preferable, but provided the solubility of the species trapped in the pore solvent is high enough, then as the system becomes concentrated during the initial stages of pre-firing, the polymeric gel may form before the solubility limit is reached. This will give a reasonably uniform distribution of the two components with the precipitate trapped in pores within the gel structure. On further heating, chemical diffusion can give rise to

TABLE I Electrical properties as a function of Ca content for films pre-treated at 300 °C

Sample $Pb_{1-x}Ca_xTiO_3$	Relative permittivity, D ($\varepsilon_r \pm$ SD)	Remanent polarization $P_r \pm$ SD ($\mu C\, cm^{-2}$)	Coercive field $E_c \pm$ SD ($kV\, cm^{-1}$)
$x = 0.1$	270 ± 25	10 ± 3.5	125 ± 25
$x = 0.15$	170 ± 10	14 ± 2	120 ± 15
$x = 0.2$	190 ± 15	10 ± 3	110 ± 30
$x = 0.25$	230 ± 10	9 ± 1	77 ± 20
$x = 0.3$	109 ± 10	7.5 ± 3	80 ± 20

Average values were calculated from 10 dot electrodes; SD = standard deviation

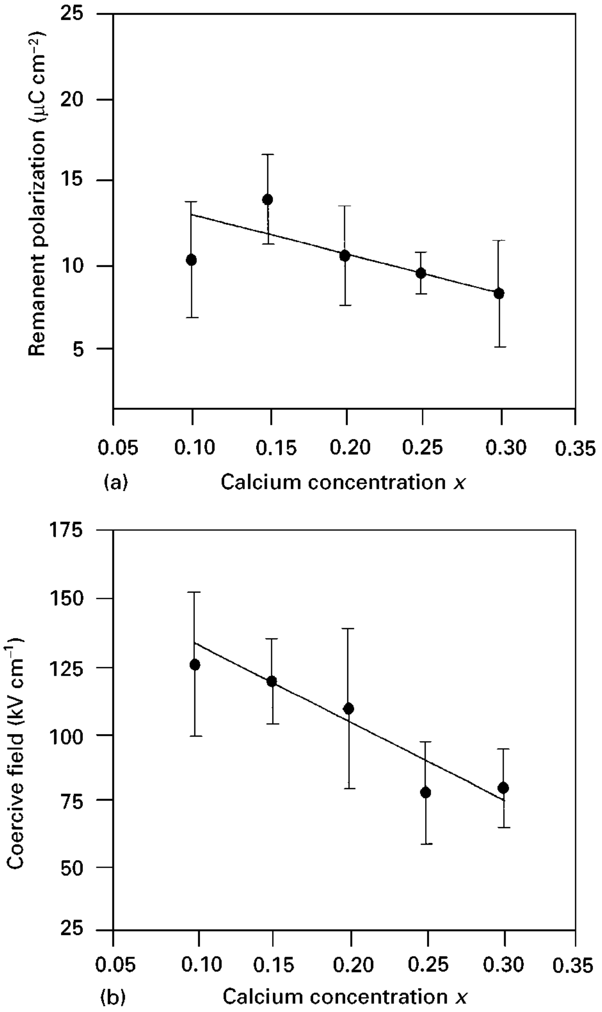

Figure 9 Variation of P_r and E_c as a function of Ca content. Error bars indicate standard deviation.

a single phase material of constant composition across the film.

4. Conclusions

A sol–gel route for synthesizing $Pb_{1-x}Ca_xTiO_3$ films has been developed by modifying a diol based route originally devised for $PbTiO_3$ and $Pb(Zr, Ti)O_3$.

Crack-free films some 0.4 μm in thickness could be formed by firing a single sol coating on $Pt/Ti/SiO_2/Si$ substrates at 650 °C. Multi-layer films were also prepared, up to a thickness of $\geqslant 3$ μm.

Ferroelectric coefficients were comparable to those reported in the literature for films made by other sol–gel routes.

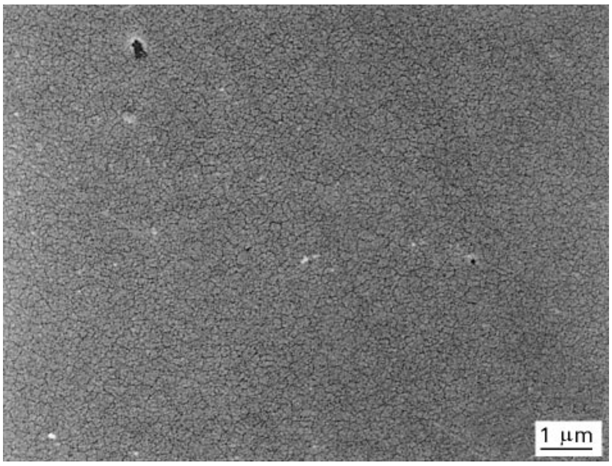

Figure 10 Example of the macro-pores, thought to be associated with the thermal decomposition process. The film was fired at 650 °C after a 230 °C hot plate treatment.

The standard deviation in these ferroelectric parameters and the incidence of electrical shorting was higher than for PZT films made by a diol sol–gel route. This seems to be linked to physical disruption in the $Pb_{1-x}Ca_xTiO_3$ films during thermal decomposition causing the formation of porosity. Variations in the distribution of porosity may account for the relatively high variations in measured electrical parameters, but chemical segregation cannot be ruled out.

Acknowledgement

S. Chewasatn thanks the Royal Thai Government for financial support.

References

1. E. YAMAKA, H. WATANABE, H. KIMURA, H. KANAYA and H. OHKUMA, *J. Vac. Sci. Technol.* **A6** (5) (1988) 2921.
2. Y. L. TU, S. CHEWASATN, R. HOLT and S. J. MILNE, In "Electroceramics", edited by W. E. Lee and A. Bell (The Institute of Materials, 1944) p. 101.
3. A. TSUZUKI, H. MURAKAM, K. KANI, K. WATARI and Y. TORII, *J. Mater. Sci. Lett.* **10** (1991) 125.
4. R. SIRERA, M. L. CALZADA, F. CARMONA and B. JIMENEZ, *ibid.* **13** (1994) 1804.
5. E. SAWAGUCHI, T. MITSUMA and Z. ISHII, *J. Phys. Soc. Jpn.* **11** (1956) 1298.
6. T. IKEDA, *ibid.* **13** (4) (1958) 335.
7. M.MCQUARRIE, *J. Amer. Ceram. Soc.* **40** (2) (1957) 35.
8. K. D. BUDD, S. K. DEY and D. A. PAYNE, *Brit. Ceram. Proc.* **36** (1985) 107.

9. C. D. E. LAKEMAN and D. A. PAYNE, *J. Amer. Ceram. Soc.* **75** (11) (1992) 3091.
10. D. C. BRADLEY, R. C. MEHROTRA and D. P. GAUR, "Metal alkoxides" (Academic Press, London, 1978).
11. N. J. PHILLIPS, M. L. CALZADA and S. J. MILNE, *J. Non-Cryst. Solids* **147** and **148** (1992) 285.
12. *Idem.*, British Patent Application 9114476.6 (July 1991).
13. M. L. CALZADA and S. J. MILNE, *J. Mater. Sci. Lett.* **12** (1993) 1221.
14. Y. L. TU and S. J. MILNE, *J. Mater. Sci.* **30** (1995) 2507.
15. G. YI. Z. WU and M. SAYER, *Ceram. Trans.* **11** (1990) 363.
16. N. J. PHILLIPS, S. J. MILNE, N. J. ALI and J. D. KENNEDY, *J. Mater. Sci. Lett.* **13** (1994) 1535.
17. N. J. ALI, P. CLEM and S. J. MILNE, *J. Mater. Sci. Lett.*, **14** (1995) 837.
18. Y. L. TU and S. J. MILNE, *J. Mater. Res.* **12** (1995) 3222.

Received 23 April
and accepted 21 May 1996